Complete solution for a two-dimensional tanh-conductivity arc

G C DAS

Department of Applied Mathematics, Indian Institute of Science,
Bangalore 560 012
Present address: Indian Institute of Astrophysics, Bangalore 560 034

Abstract. This paper is a sequel to an earlier work on the dynamics of a two-dimensional tanh-conductivity arc. We present here a complete solution, based on the Galerkin technique, for the characteristic variation of current-voltage through an arc. The present results are qualitatively very similar to those obtained in earlier theoretical and experimental studies. The solutions obtained are the modification of the basic equations, which has led to quantitative investigations of the present problem. The influence of various arc parameters on the arc formation is also discussed.

Keywords. Arc; Galerkin method; tanh-conductivity.

1. Introduction

In recent years, a great deal of interest has been focussed on the advantages of the dynamics of arc phenomena. Many investigators have tried to get an insight into the basic mechanism of arc discharges but most of them have chosen an ideal model for the sake of mathematical simplicity. In this paper we attempt to study the basic mechanism of arc discharges in a two-dimensional tanh-conductivity arc. Due to the inherent limitations of the numerical procedure, an earlier study (Ayyaswamy et al 1978) of a two-dimensional tanh-model arc lead to an incomplete solution of the current-voltage variation. Further study of the arc was necessitated by modifying the basic equations governing the arc dynamics. We consider here a two-dimensional planar arc between two planar electrodes. The mathematical formulation of the model is very similar to that for the discharge lamps presented by Waymouth (1971). With the knowledge gained in our earlier work (Ayyaswamy et al 1978) the basic equations are now modified. We also study the equal and unequal temperatures of the cathode and anode. The results obtained here are similar to those obtained in another experiment on arc discharge lamps (Waymouth 1971).

2. Mathematical formulation of the problem

We consider a simplified model of a planar arc between two planar electrodes. Figure 1 shows the geometry, boundary conditions and co-ordinate systems of the arc. In the absence of radiation and convection, the fundamental equation for the energy conservation in the arc is given by the Elenbass-Heller equation,
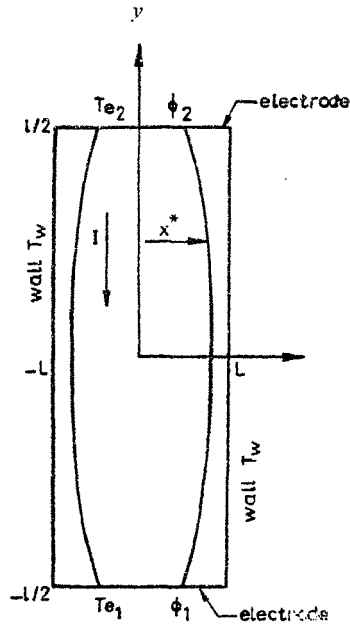
$$\nabla (k \nabla T) = -JE, \tag{1}$$

Figure 1. Arc geometry, boundary conditions and co-ordinate system.

where k is the thermal conductivity; T is the temperature; J is the current and E is the electric field. Equation (1) is supplemented by Ohm's law: $J = \sigma E$, where σ is the electrical conductivity assumed to be a function expressed by a tanh-function proposed first by Whitman *et al* (1976). Further $\nabla \times E = 0$ i.e. $E = -\nabla \phi$, where ϕ is the electrostatic potential. We introduce the heat flux S as

$$S(T) = \int_0^T k(T')\, dT'. \tag{2}$$

With the definition of S, the electrical conductivity $\sigma(S)$ is expressed as:

$$\sigma(S) = \tfrac{1}{2}\sigma_* \{1 + \tanh\,[a(S - S_*)]\}, \tag{3}$$

where σ_* and a are material constants. The basic equations are subjected to the following appropriate boundary conditions:

$$x = \pm L, \quad S = S_w,\ \partial\phi/\partial x = 0, \tag{4}$$
$$y = \pm l/2, \quad S = S_{c,a}\,(x),\ \phi = \phi_{c,a}.$$

The total current through the arc is given by

$$I = \int J\,(\hat{j}\,d\,A)$$

(where dA is the cross-sectional area) which can be represented after straightforward manipulation as:

$$\bar{I} = -\tfrac{1}{2} \int_{-1}^{\bar{1}} \left[1 + \tanh\,(\mu\,\bar{S})\,\frac{\partial\bar{\phi}}{\partial\bar{y}}\,d\bar{x} \right], \tag{5}$$

where $\bar{S}$ is the non-dimensional quantity defined as $\bar{S}=(S-S_*)/(S_*-S_w)$. The other parameters are normalised as:

$$\bar{x} = x/L, \quad \bar{y} = y/L,$$

$$\mu = a(S_w-S_*), \ b = l/2L,$$

$$\bar{I} = I[2 \ \sigma_* \ (S_*-S_w)]^{-\frac{1}{2}},$$

$$\bar{\phi} = \phi[2 \ (S_*-S_w)/\sigma_*]^{-\frac{1}{2}}.$$

The basic non-dimensional equations are now read as:

$$\frac{\partial^2\bar{S}}{\partial\bar{x}^2}+\frac{\partial^2\bar{S}}{\partial\bar{y}^2} + [1+\tanh(\mu\bar{S})] \ [(\partial\bar{\phi}/\partial\bar{x})^2 + (\partial\bar{\phi}/\partial\bar{y})^2] = 0, \tag{6}$$

$$\frac{\partial^2\bar{\phi}}{\partial\bar{x}^2}+\frac{\partial^2\bar{\phi}}{\partial\bar{y}^2} + \mu[1-\tanh(\mu\bar{S})] \left[\frac{\partial\bar{\phi}}{\partial\bar{x}}\frac{\partial\bar{S}}{\partial\bar{x}}+\frac{\partial\bar{\phi}}{\partial\bar{y}}\frac{\partial\bar{S}}{\partial\bar{y}}\right] = 0, \tag{7}$$

and the corresponding boundary conditions are:

$$\bar{x} = \pm 1, \quad \bar{S} = -1, \quad (\partial\bar{\phi}/\partial\bar{x}) = 0,$$

$$\bar{y} = \pm b, \quad \bar{S} = \bar{S}_{c,a}(\bar{x}), \ \bar{\phi} = \bar{\phi}_{c,a}. \tag{8}$$

Equations (6) and (7) are solved, though not completely, with boundary conditions (8). But, the current-voltage variation in a certain range of the discharges is not fully obtained (Ayyaswamy *et al* 1978).

The solution of $\bar{\phi}$ obtained by Ayyaswamy *et al* (1978) shows that $\bar{\phi}$ remains almost constant with respect to $\bar{x}$. The solution of $\bar{\phi}$ allows us to assume $\bar{\phi}$ to be a constant with respect to $\bar{x}$. Consequently the assumption modifies the basic equations and can be read as (the bar is omitted hereafter):

$$(\partial^2 S/\partial x^2) + (\partial^2 S/\partial y^2) + [1+\tanh(\mu S)] \ (\partial\phi/\partial y)^2 = 0, \tag{9}$$

and $\qquad I = -\frac{1}{2} \ (\partial\phi/\partial y) \int_{-1}^{1} \ [1+\tanh(\mu S)] \ dx. \tag{10}$

To solve equation (9) together with (10) and the boundary conditions (8), we introduce the new variables $u(x, y)$ for $S(x, y)$ as:

$$S(x, y) = u(x, y) + F(x, y), \tag{11}$$

where $\qquad F(x, y) = [f_c(x)+1] \left(\frac{y+b}{2b}\right) - [f_a(x)+1] \left(\frac{y-b}{2b}\right) - 1, \tag{12}$

$f_c(x)$ and $f_a(x)$ are respectively cathode and anode temperature parameters defined as

$$f_{c,a}(x) = f_{2,1}^{1}(1-x^2)^2 - 1, \tag{13}$$

where f_2 and f_1 are numerical constants. Equations (9) and (10), with the help of (11) can be rewritten as:

$$\mathscr{L}\{\mu, \phi\} \equiv \frac{\partial^2 u}{\partial x^2} + \frac{\partial^2 u}{\partial y^2} + \frac{\partial^2 F}{\partial x^2} + [1 + \tanh \mu(u+F)](\partial\phi/\partial y^2) = 0, \qquad (14)$$

and

$$I = -\tfrac{1}{2}(\partial\phi/\partial y)\int_{-1}^{1} \{1 + \tanh[\mu(u+F)]\}dx, \qquad (15)$$

and the boundary conditions are

$$x = \pm 1, \qquad u = 0, \qquad (16)$$

$$y = \pm b, \qquad u = 0,$$

$$\frac{\partial u}{\partial x}(0, y) = 0.$$

To solve the above equations for the prescribed arc parameters, with the homogeneous boundary conditions, we adopt the Galerkin procedure (Finlayson 1972); u is expanded into an approximating series of polynomials *viz.*:

$$u(x, y) = \Sigma_m \Sigma_n \Sigma_p (1-x^2)^m (1-t^2)^n t^p, \qquad (17)$$

where $t = y/b$. The number of terms in the series has to determine the accuracy of percentage to be imposed on the obtained results. Using the expanded expression (17) in (14), we form the integral

$$I_{mnp} = \int_{-b}^{b} dy \int_{-1}^{1} \mathscr{L}\{u, \phi\} (1-x^2)^m (1-t^2)^n t^p dx. \qquad (18)$$

Since we now require the residuals to be orthogonal to each term in the approximating series, we make $I_{mnp} = 0$, which gives a set of $m \times n \times p$ equations. Initially, we consider a series with four terms but, whenever necessary, we consider the series with eight terms. In the case of unequal electrode temperatures, a series of eight terms is considered. The iteration on the Galerkin coefficients A_{mnp} is continued until the condition

$$\left| [A_{mnp}^{r+1} - A_{mnp}^{(r)}]/A_{mnp}^{(r+1)} \right| < 10^{-2}, \qquad (19)$$

is satisfied. The results obtained by the procedure described above agree well with the experimental results on electric discharge lamps (Waymouth 1971). To check the present results for a few cases, we consider more terms in the series, but they do not show a very significant variation from the results obtained with the series of eight terms. After obtaining satisfactory values of the Galerkin coefficients A_{mnp} we calculate the heat flux potential and the arc shape from the expression of S. We also obtain the net heat transfer to the walls as well as to the electrodes from the

arc. The dimensionless heat transfer rates to the wall Q_w and to the electrodes $Q_{a,c}$ are computed respectively from the following expressions:

$$Q_w = -b \int_{-1}^{1} (\partial S/\partial x)_{x=1} \, dt, \tag{20}$$

$$Q_{a,c} = \pm \int_{-1}^{1} (1/b) (\partial S/\partial t)_{t=\pm 1} \, dx, \tag{21}$$

where Q_a and Q_c represent the heat transfer to the anode and to the cathode respectively and have been made dimensionless by $L(S_* - S_w)$.

3. Discussion

Figure 2 shows the dimensionless current-voltage variation for the different aspect ratios b and for the case of electrodes having equal and unequal temperatures. The figure clearly shows that it is necessary to operate with the hot electrodes for an arc to be formed between the two electrodes. In the case of comparatively cold electrodes, the current-voltage variation exhibits three distinct phases. In the initial stage, where the current is very small (part AB: only curve 5 is marked), the current increases with the voltage, but does not have any significant effect on the electrodes. The current remains almost unchanged. This characterisation is continued until the whole electrodes are heated and are at a high voltage. Consequently in this range, the arc is not fully formed. The range described above is widened with the increase of the distances between the electrodes and consequently more voltage is required to form the arc. For a fixed arc geometry with prescribed electrode temperatures, it is necessary to input a sufficient voltage/current to arrive at a new region
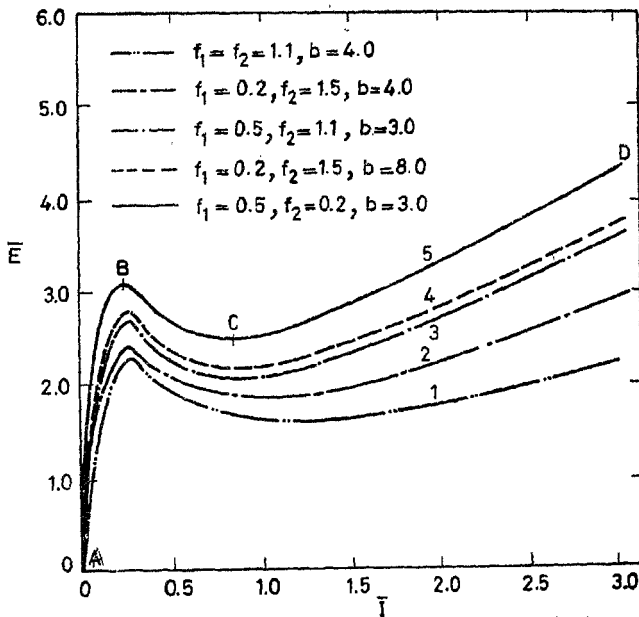

Figure 2. Current voltage characteristics for $\mu = 2$.

(part *CD*) for which an arc is formed between the two planar electrodes. The current in this region varies linearly with the voltage. Between the above two distinct ranges (*AB* and *CD*) there is a transition range (part *BC*) whose existence depends mainly on the electrode temperatures. In this region, the current-voltage variation shows an opposite tendency. In the case of the hotter electrodes this region does not exist or may exist only insignificantly. However, for the cold electrodes, part *BC* will exist between the electrodes. The electrode distance has also a role in the formation of the *BC* part of the curve.

Figure 3 shows the variation of heat flux potential distribution with $\bar{y}/b$ along the central line ($\bar{x}=0$) and with $\bar{x}$ perpendicular to the central line ($\bar{y}/b=0$). The figure shows that whenever the heat fluxes are negative the arc is not formed. In order to have an arc, the first criterion is that the heat flux potential should be positive. The arc can have an insignificant formation, provided the temperature parameters of the electrodes exceed one. Otherwise, the arc boundary will not cover any part of the surface of the electrode. We have considered the following temperature parameters for our numerical calculation:

(1) $f_1 = f_2 \quad = 1\cdot1, \ b = 4\cdot0,$

(2) $f_1 = 0\cdot2, f_2 = 0\cdot5, \ b = 4\cdot0.$

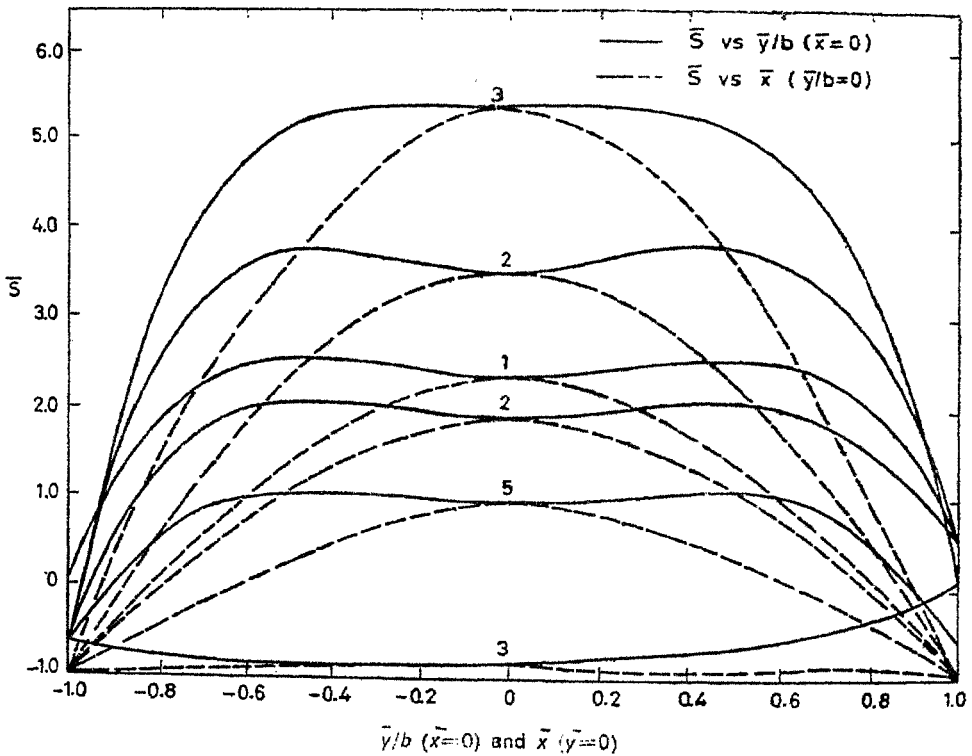(3) $f_1 = 0\cdot5, f_2 = 1\cdot1, \ b = 3\cdot0,$

Figure 3. Temperature profiles on arc. $\bar{I}$ is the parameter of the curves 1, 2, 3 and 5.

(4) $f_1 = 0.2, f_2 = 1.5, b = 8.0,$

(5) $f_1 = 0.5, f_2 = 0.2, b = 3.0,$

and the respective curves are 1, 2, 3, 4 and 5 in figure 2. In the case (5), no arc can be formed to cover any part of the electrodes. Cases (2)–(4) show that the arc surface if formed distinctly, will only touch the cathode. But in the case of (1), the arc surface will touch both the cathode and the anode. Figure 4 shows the variation in the arc shape corresponding to the characteristic curves 1, 2, 3 and 5 given in figure 2. The arc shape is defined by the locus of the points for which $\bar{S}=0$. In the range in which the current contribution is small, or the electrodes are cold (i.e., the region AB), $\bar{S}$ is always negative which shows that no arc is present between the electrodes. In the case of high current or voltage, there is an arc formation. The thickness of the arc will be broadened with increasing current. It indicates that due to the high current input, the arc surface almost touches the walls. Thus, it is necessary to control the arc shape in order to make a full use of the arc for lighting purposes. When an external mechanism is used to control the arc shape, the arc will exhibit great brightness even though the input current is comparatively small.

The variation of the heat transfer phenomena is shown in Figure 5. In the low current region, the electrodes always lose heat which are absorbed by the walls. The walls thus gain more and more heat with increase of the current and electrodes continue to lose that heat until the arc is formed. This happened in the branch curve AB. In the second branch of curves in figure 2, either the cathode or anode will lose the heat depending on the initial temperatures of the cathode and the anode. The low temperature electrode will gain heat from the higher temperature electrode.

In our calculation, we assume that the cathodes always have the higher temperature. So the walls and the anode will always absorb the heat. On the other hand if the cathode is colder than the anode, the cathode will absorb and the anode will lose the heat. But a different feature is observed as soon as the arc is formed. If a complete arc between the planar electrodes is formed, then both the walls and the electrodes will be heated by the arc. The heat transfer increases with the
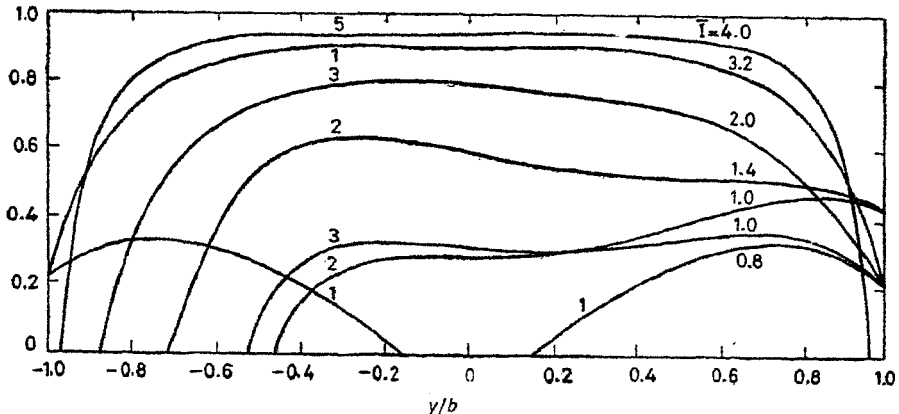

Figure 4. Arc shape: x^* versus $\bar{y}/b$. $\bar{I}$ is the parameter of the curves 1, 2, 3 and 5.
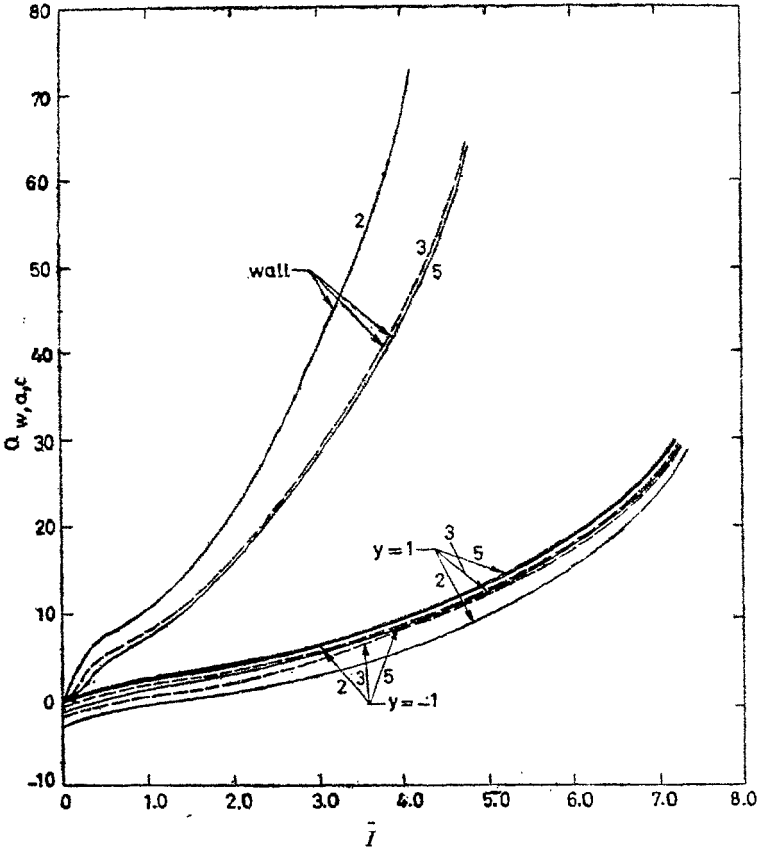
Figure 5. Heat transfer to walls ($\bar{x} = \pm 1$) and electrodes ($\bar{y}/b = \pm 1$). $\bar{I}$ is the parameter of the curves 2, 3 and 5.

current. At a high current, a dramatic feature of heat transfer will be exhibited i.e., the boundaries of the arc will attain the maximum volume and almost touch the walls and this explains the fact that heat transfer to walls will be of a high order. Similarly, at a high current, the electrodes will gain heat from the arc.

4. Conclusion

By using the Galerkin technique a complete solution for a system of nonlinear differential equation governing the arc phenomena between the two electrodes is obtained. The characteristic features of the current-voltage variation show a good agreement between theory and experiment. The classic behaviour of the arc, emerging from our theoretical study, is summarised as follows. In the case of cold electrodes, a high current/voltage is necessary to form an arc between two electrodes, whereas high temperature electrodes require only a small current. In the case of a high current, the arc boundaries almost touch the walls due to which the arc loses a large amount of heat to the walls. So it is necessary to develop a mechanism to

control the arc shape and due to this, a high intensity arc can be formed. Our mathematical modelling of the arc phenomenon also concludes that the higher electrode distance requires a higher voltage to sustain the arc between the electrodes. In the case of a lower current, the walls gain heat always from the electrodes but there is a region in which the hotter electrodes lose the heat to the walls and to the cold electrodes. As soon as the arc is formed, both the walls and the electrodes gain heat from the arc.

References

Ayyaswamy P S, Das G C & Cohen I M 1978 *J. Appl. Phys.* **49** 160
Finlayson B A 1972 *The method of weighted residuals and variational principles* (New York: Academic Press)
Waymouth J F 1971 *Electric discharge lamps* (Massachusetts: MIT Press)
Whitman A M, Ayyaswamy P S & Cohen I M 1976 *J. Appl. Phys.* **47** 4827